

Geochemistry, mineralogy and plate tectonic setting of a Late Cretaceous Sn–W Granite from Sumatra, Indonesia

M. C. G. CLARKE

Overseas Directorate, British Geological Survey, Keyworth, Nottingham NG12 5GG, England

AND

B. BEDDOE-STEPHENS*

Geochemistry Directorate, British Geological Survey, Murchison House, West Mains Road, Edinburgh EH9 3LA, Scotland

Abstract

The Hatapang granite was discovered during geological mapping and mineral exploration in northern Sumatra by the British Geological Survey in conjunction with the Indonesian Directorate of Mineral Resources. The pluton comprises a two-mica granite which shows significant greisenization and veining around its margins associated with Sn and W mineralization. An Rb–Sr isochron derived for the pluton indicates an age of 80 Ma and an initial $^{87}\text{Sr}/^{86}\text{Sr}$ ratio of 0.7151. This together with major and trace element data show the Hatapang to be of clear S-type affinity.

The greisens are quartz–mica–topaz rocks and are almost totally deficient in Na. Trioctahedral mica compositions progress from biotite through siderophyllite to zinnwaldite during final differentiation and greisenization of the granite. Accompanying dioctahedral micas are phengitic. Associated with late-stage differentiation of the granite is the precipitation of tourmaline and various Nb–Ta oxides. Sn and W mineralization is manifested as cassiterite in the greisens, while wolframite tends to be related to quartz veining. A later and lower temperature sulphide event produced a suite of base metal sulphides and Ag–Bi–Pb sulphosalts. The identification of a Sn–W granite of Cretaceous age in northern Sumatra provides a link with occurrences of economically important Late Cretaceous Sn–W granites in Thailand and Burma and increases the potential of an area which until recently was thought to lie outside the SE Asian tin belt.

KEYWORDS: granite, tin, tungsten, geochemistry, mineralogy, plate tectonics, Sumatra

Introduction

THE Hatapang granite was first located in 1979 during a regional geological and geochemical reconnaissance of Sumatra north of the equator. This was carried out as a technical cooperation project between the British Geological Survey and the Indonesian Directorate of Mineral Resources. Details of the project are given by Page *et al.* (1978) and a summary account of the geology by Cameron *et al.* (1980). Results of the stream sediment geochemical survey are available in atlas form for 15 elements at 1:2 500 000 (Stephenson *et al.*, 1982)

and a preliminary account of Sn regional geochemistry is reported by Johari *et al.* (1981). The regional setting of the Hatapang pluton is described by Clarke *et al.* (1982), and the results of follow-up field investigations are given by Hamidsyah and Clarke (1982).

This paper describes the geochemistry and mineralogy of the granite and mineralized rocks and the significance of the pluton in relation to the SE Asian tin province.

Geologic setting

The present day geology of Sumatra is dominated by a volcanic arc and major trans-

* Author for correspondence.

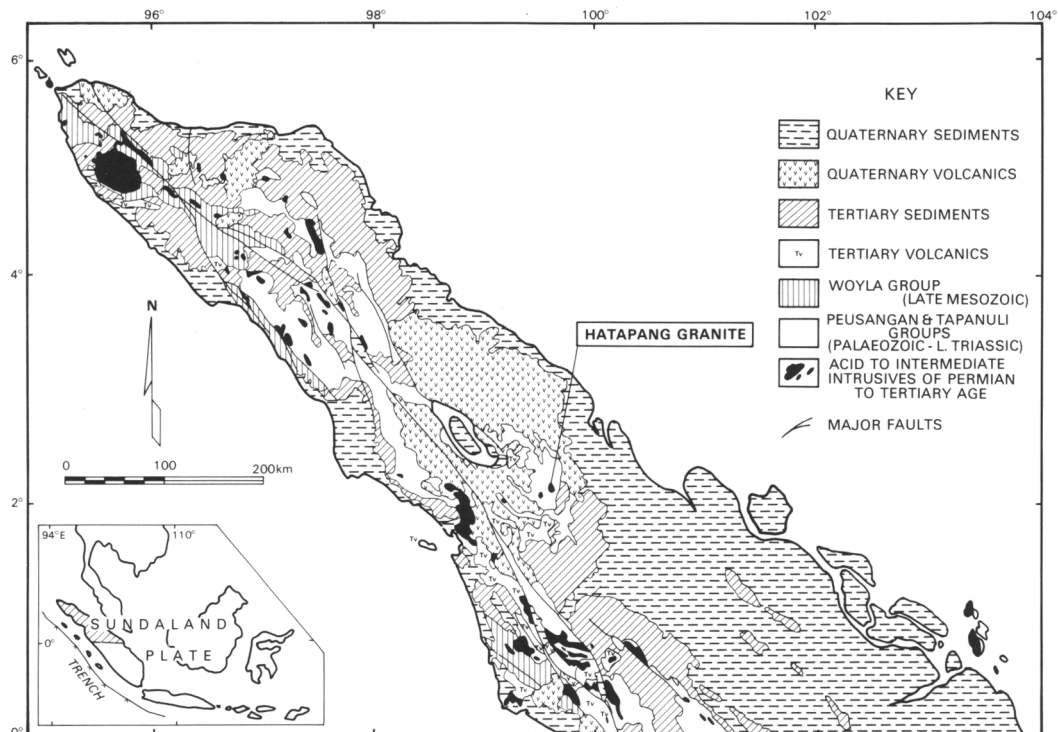


FIG. 1. Outline geology of north Sumatra showing the location of the Hatapang pluton. Inset shows site of current subduction.

current fault system (Sumatra Fault Zone) running the length of its western edge (Fig. 1). This is related to the oblique, northward subduction of Indian oceanic crust beneath Sumatra. Lying to the east of the geanticline, along which subduction related activity has occurred intermittently since the Late Triassic at least, is the present-day back arc terrain containing Tertiary basinal sequences which are often prolific oil producers. At the latitude of the Hatapang pluton (Fig. 1), this Tertiary cover has been partly removed due to uplift in the Quaternary and the Carboniferous-Triassic basement exposed. It is into this basement that the Hatapang granite was emplaced.

The basement rocks, belonging to the Tapanuli Group, consist of a thick sequence of greywackes and diamictites which are similar to and correlate with formations in mainland SE Asia, all of which are of probable Gondwana affinity (Cameron *et al.*, 1980; Metcalfe, 1983). The diamictites are usually unbedded, unfossiliferous and sometimes contain pebbles and cobbles of granite, gneiss, marble and quartzite, all of which indicate a continental provenance.

Within 0.5–1.0 km of the contact the Tapanuli wackes show evidence of thermal metamorphism with the development of siliceous black hornfels. Closer to the granite the hornfels assumes a purply brown colouration due to biotite growth. In addition some skarnification and epidotization of calcareous horizons occur.

The outcrop pattern of the Hatapang pluton is shown in Fig. 2, along with sample localities and observed mineralization. It should be noted that the area is covered by virgin rain forest and access and outcrop is limited to stream courses. Consequently the pluton could not be sampled systematically and some indications of mineralization are based on examination of float.

Description of the rocks and their inter-relation

Granite. The granite making up the bulk of the pluton appears to be texturally uniform and, as shown by modal analyses, occupies a small area in the 'granite' field shown in Fig. 3 (Streckeisen, 1976). It is mildly porphyritic with orthoclase pheno- or megacrysts up to 4 cm long, set in a

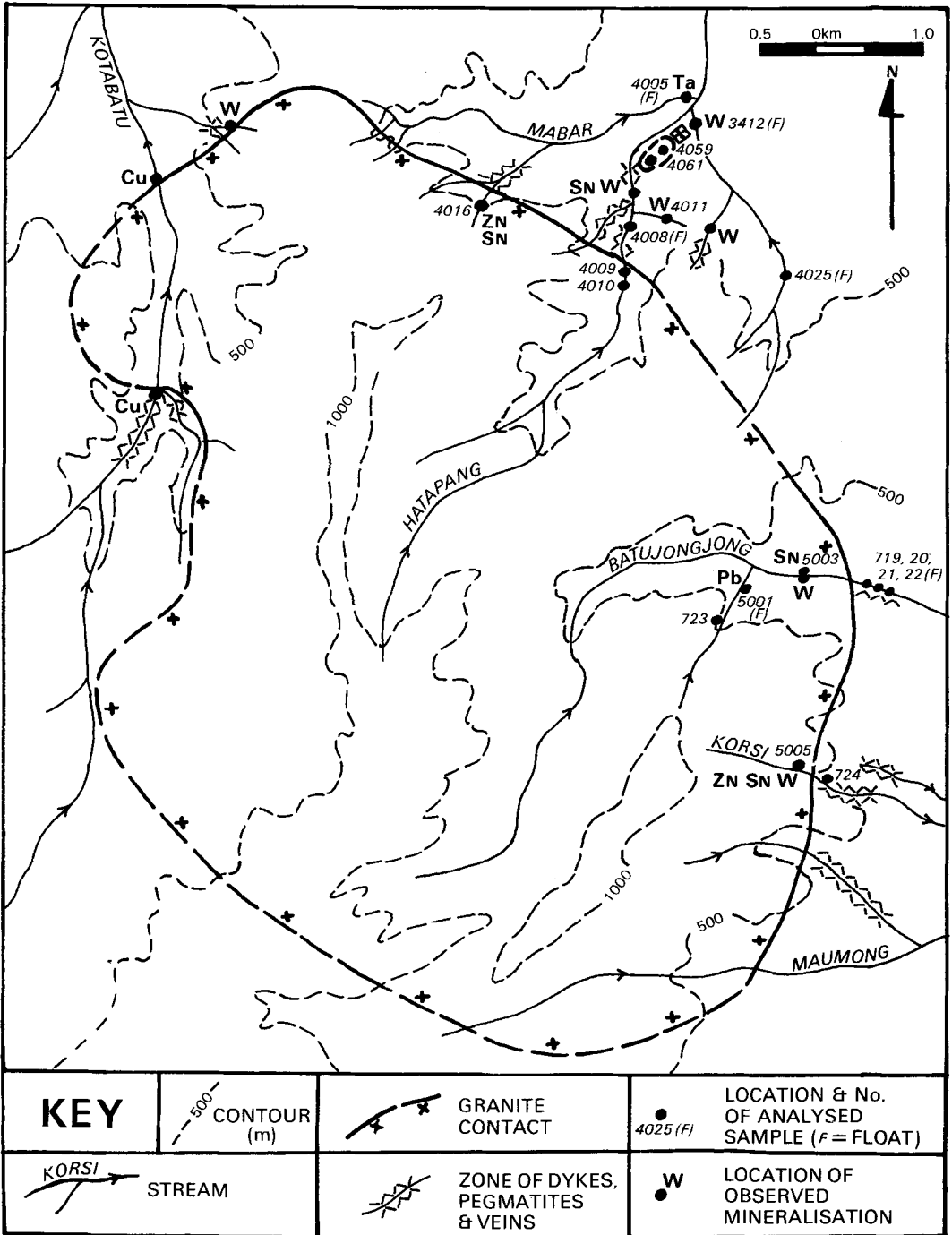


FIG. 2. Outcrop pattern of the Hatapang pluton showing location of samples and observed mineralization.

medium grained groundmass which includes biotite and subordinate muscovite. Tourmaline is common, occurring in sub-metre sized patches or in elongate pegmatitic segregations within the granite. Concentrations of blue-green beryl occasionally accompany black tourmaline. These pegmatites are not associated with noticeable alteration and no significant mineralization has been noted in them.

The orthoclase phenocrysts are partly perthitic and the groundmass is variably altered. In particular, K-feldspar is often cloudy or replaced by fine sericite. The only mafic phase present is brown biotite which is occasionally interleaved with, or replaced by, muscovite. Muscovite also forms clear pools interstitial to feldspar and quartz. Chloritization of both biotite and muscovite is sometimes advanced and can be correlated with the degree of feldspar alteration. Interstitial tourmaline, fluorite and topaz are late crystallization products and indicate the presence of residual F- and B-rich fluids. Common accessory phases include zircon, monazite, rutile and apatite. Ilmenorutile, ixiolite, samarskite and thorite have also been noted.

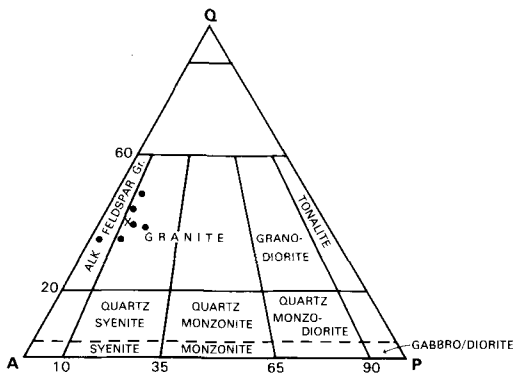


FIG. 3. Modal analyses of six granite samples plotted in the classification diagram recommended by Streckeisen (1976). Average composition indicated by \times .

Marginal granite zone. Within a few tens of metres, but occasionally up to 100 or more metres of the contact, the pluton is extremely heterogeneous with several phases of microgranite and aplite veining and extensive patches of pegmatite. Tabular greisens up to 30 cm in thickness also occur and grade into unaltered granite. These usually border quartz veins (up to 4 cm width) and are greyish with conspicuous alteration of biotite to grey-green or bronzy mica. The greisen-bordered veins sometimes occur in sub-parallel swarms and can contain easily visible wolframite and arsenopyrite.

The greisens are characterized by the assemblage quartz, topaz, mica and fluorite. Feldspar is absent in general except for occasional veinlets of pink K-feldspar. Quartz is in part relict from the granite protolith but shows a degree of recrystallization and euhedral overgrowth. Mica forms in a variety of textures from interstitial aggregates to well-formed radial sheaves and large single crystals. Two micas can be present, a colourless muscovite and a near colourless, greenish or brownish trioctahedral mica. The compositions of these minerals are discussed below. Topaz tends to form clusters of rounded grains while fluorite is anhedral and interstitial.

The main metalliferous phase in the greisens is cassiterite, which forms aggregates up to several millimetres across. There is usually good crystal face development adjacent to mica, and brown, yellow and colourless growth banding is distinct. Rare wolframite also occurs in the greisens. Sulphide minerals comprise locally abundant chalcopyrite and arsenopyrite, lesser amounts of pyrite and sphalerite and minor amounts of cosalite, gustavite, bismuthinite and galena. Crystallization of the sulphides, in particular the Pb-Bi phases, is controlled by grain boundaries and cleavage planes and indicates a lower temperature and later mineralization event.

Quartz veins within the granite are usually greisen-bordered, as noted, and can contain a similar mineral assemblage, although with excessive quartz compared to the greisens. Wolframite tends to occur rather than cassiterite and is often associated with arsenopyrite. The phases aikinite and wittichinite were identified in one vein along with pyrite, sphalerite and chalcopyrite. Other veins are not greisen-bordered, have only a thin argillic alteration zone and contain insignificant fluorine minerals. These veins may be barren or contain Cu, Pb and Zn sulphides only. Finally some veins show features of both the above types and show evidence of multiphase development.

Marginal country rock zone. The effects of veining and alteration as well as extending into the pluton also occur up to several hundred metres beyond the contact. Granite, microgranite and pegmatite veins or dykes, up to several metres wide, are numerous in this zone. They display little alteration of adjacent sediments and are unmineralized, though in the SW area of the pluton tourmaline is prominent in some of these dykes.

In addition there is a suite of narrower (< 10 cm) veins that can be related spatially to the endocontact greisen-bordered veins described above. These are generally quartz-muscovite veins with wolframite and arsenopyrite being the most prominent metalliferous phases. Cassiterite may be present but

is subordinate and not associated with wolframite. Strong alteration zones border these veins with the development of biotite and muscovite-rich selvages. Pyrite, chalcopyrite and tennantite also occur. Similar but millimetre-sized veinlets extend for up to 1 km from the pluton and display selvages 5–10 times the vein width, indicative of the reactivity of the vein fluids.

Geochemistry

Seventeen rocks were analysed, ten granites unaffected by greisenization (Table 1), four greisens and three mineralised veins (Table 2).

Granite. All the granites plot in a restricted and evolved compositional field, close to the thermal minimum in the An–Ab–Or–H₂O–F system, Fig. 4

TABLE 1. Granite Analyses

Wt%	4039	4059	4061	5001	M0719	M0720	M0721	M0722	M0723	M0724
SiO ₂	77.5	75.2	72.9	75.45	74.75	75.72	75.03	77.81	75.17	75.37
TiO ₂	0.08	0.13	0.19	0.07	0.11	0.10	0.11	0.08	0.20	0.07
Al ₂ O ₃	12.7	13.8	14.8	12.91	13.42	13.02	13.32	12.20	12.81	13.01
Fe ₂ O ₃	0.53	0.44	0.51	2.32*	0.35	0.76	0.25	0.06	0.75	0.12
FeO	0.94	1.27	1.21	–	1.28	0.70	1.34	1.08	1.03	1.13
MnO	0.03	0.06	0.04	0.03	0.00	0.00	0.00	0.00	0.00	0.00
MgO	0.2	0.3	0.4	0.28	0.11	0.12	0.13	0.08	0.25	0.07
CaO	0.9	0.3	1.1	0.48	1.02	0.87	1.02	0.77	1.23	0.83
Na ₂ O	3.1	2.9	3.0	3.47	3.46	3.17	3.48	3.27	2.99	3.44
K ₂ O	4.6	5.5	5.8	4.34	4.97	5.01	4.78	4.55	4.70	4.80
P ₂ O ₅	0.06	0.04	0.10	0.05	0.01	0.02	0.03	0.01	0.04	0.01
F	0.37	0.46	0.27	0.14	0.57	0.53	0.55	0.44	0.34	0.40
S	0.13	0.13	0.10	0.00	0.01	0.01	0.01	0.01	0.00	0.00
LOI	0.69	0.68	0.73	0.52	0.99	0.74	0.87	0.62	0.77	0.68
O=F	0.16	0.19	0.11	0.06	0.24	0.22	0.23	0.19	0.14	0.17
Total	101.67	101.02	101.04	100.00	100.82	100.55	100.69	100.79	100.14	99.76

Trace elements (ppm)

Li	192	506	168	34	237	209	185	166	118	204
Be	5	17	11	5	7	140	21	8	13	8
B	254	9	53	7	26	31	38	21	426	16
Cl	5	80	10	ND						
Cu	<1	4	1	8	4	3	4	11	5	6
Zn	88	53	41	33	31	29	42	24	15	39
Ga	17	22	22	19	17	18	17	18	14	18
Rb	650	1110	580	629	676	762	617	724	514	723
Sr	31	45	47	12	12	14	12	11	61	11
Y	70	15	20	159	190	139	254	178	63	215
Zr	115	160	150	121	184	100	187	179	222	145
Nb	35	30	60	45	63	44	80	60	29	53
Mo	<3	<3	<3	<3	<3	<3	<3	<3	<3	<3
Ag	<1	<1	<1	<1	<1	<1	<1	<1	<1	<1
Cd	<1	<1	<1	<1	<1	<1	<1	<1	<1	<1
Sn	85	130	50	47	16	39	50	17	28	15
Ba	74	116	184	92	29	39	34	21	191	41
La	<30	45	60	40	85	60	85	50	80	40
W	35	10	12	33	31	29	42	24	15	39
Pb	75	75	80	240	61	76	69	76	56	91
Bi	<10	<10	<10	16	16	8	11	10	10	12
Th	70	75	80	59	86	47	98	76	80	54
U	15	10	15	22	31	26	41	31	19	26

Notes: Major oxides determined by Direct electron-excitation XRS, Trace elements by XRF and OES. ND = Not determined. * Total Fe

TABLE 2. Greisen and quartz vein analyses

wt%	4008G	4010G	40256	5003G	5005G	4011V	4016V
SiO ₂	72.7	76.1	69.7	70.80	79.11	54.07	84.1
TiO ₂	0.01	-	0.02	-	-	0.07	0.02
Al ₂ O ₃	10.2	11.3	11.9	13.28	11.59	2.63	2.1
Fe ₂ O ₃	2.00	6.02*	1.50	8.35*	1.50*	23.22*	1.37*
FeO	1.99	-	4.25	-	-	-	-
MnO	0.12	0.11	0.42	0.16	0.04	0.06	-
MgO	0.1	0.1	0.1	0.14	0.16	0.31	0.1
CaO	0.5	0.5	0.4	0.27	1.71	0.56	1.6
Na ₂ O	-	-	-	-	-	0.05	0.1
K ₂ O	3.4	3.9	2.4	1.15	2.04	0.63	0.8
P ₂ O ₅	0.53	0.02	0.03	0.03	0.03	0.26	0.03
F	0.46	0.52	2.30	1.89	1.90	0.26	0.64
S	0.10	0.81	0.17	1.13	0.02	6.92	0.58
LOI	1.61	2.10	1.23	3.04	1.86	12.75†	0.90
O F	0.19	0.22	0.97	0.79	0.80	0.11	0.27
Total	99.78‡	100.45	99.81‡	99.40	99.18	101.05	99.06‡

Trace elements (ppm)

Li	524	207	>1000	230	150	18	12
Be	2	3	3	1	2	2	166
B	<7	10	<7	<7	8	<7	25
Cl	10	35	80	ND	ND	ND	5
Cu	37	1280	9	666	1880	381	447
Zn	98	114	127	140	60	20	>2500
Ga	21	27	30	11	8	2	6
Rb	1390	1690	1530	495	587	134	160
Sr	<1	1	2	1	1	<1	1
Y	<10	60	<10	46	120	<10	80
Zr	45	80	65	61	87	10	50
Nb	320	35	300	19	121	95	420
Mo	<3	<3	<3	32	<2	10	6
Ag	<1	6	<1	10	3	1	3
Cd	<1	<1	<1	ND	ND	ND	7
Sn	5.32%	270	5.01%	619	3.65%	4044	5.51%
Ba	<1	<1	<1	<1	1	<1	<1
La	<30	<30	<30	<30	<30	<30	<30
W	110	30	115	92	686	2.1%	415
Pb	95	40	110	259	32	10	2070
Bi	20	40	10	52	234	289	1400
Th	15	35	30	25	45	8	<10
U	15	25	15	23	13	3	25

* total Fe. † Total includes Sn as SnO₂. ‡ Contains significant As from arsenopyrite. G - Greisen V - Vein.

(Manning *et al.*, 1980). Given the average content of F in the granites (0.5%), which is several times the granitic average, the P_{fluid} of crystallisation derived from Fig. 4 is probably less than 1 kbar and temperatures of consolidation at or less than 700°C. This indicates an epizonal setting for the pluton (i.e. < 3 km depth).

Trace elements differ significantly from average

granite values as derived by, for example, Taylor, 1964 (Fig. 5). Sr and Ba are lower while the lithophile elements Li, Be, B, Rb, Th, U and Nb are considerably enriched. Sn and W are also enriched whereas the chalcophile elements such as Cu, Zn, Ag and Bi are close to or less than average.

Greisen. Compared with the granites from which they are formed, the greisens have slightly lower

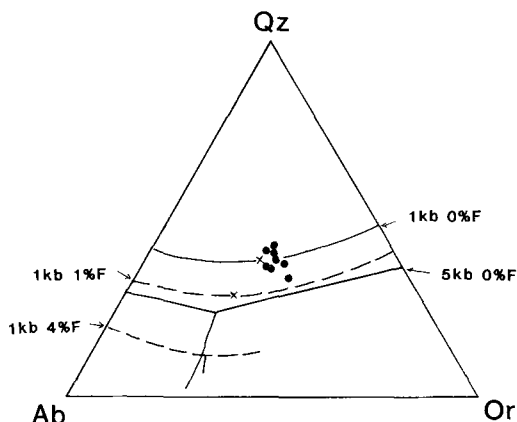


FIG. 4. Projection of the analysed granites into the Q-Ab-Or-H₂O-F system. Phase boundaries taken from Manning *et al.* (1980). × = positions of thermal minima.

Al₂O₃ and K₂O, but most noticeable is the almost total lack of Na₂O (Table 2). This correlates with

the absence of feldspar, particularly plagioclase, and indicates that during feldspar breakdown Na was efficiently leached from the rock.

Trace elements are variable (Fig. 5), with Sn reaching percent levels due to cassiterite precipitation. Li values are similar to those of the granite except in one sample (4025) where over 1000 ppm (the upper determination limit, see Table 2) is present. The elements B and Be are depleted relative to unaltered Hatapang granite, but these elements are characteristically fixed in tourmaline and beryl in the pegmatitic stage of granite crystallization. Rb shows a trend toward enrichment in the greisens. This probably represents the preferential partitioning of Rb into mica compared to K-feldspar, as suggested by Groves (1972). Ba, by contrast, while it can easily substitute for K in mica has been, like Na, effectively leached from the system. The elements Nb and W (and probably Ta) have all increased in the greisen, probably due to fixation in wolframite and cassiterite. Other HFS incompatible elements such as Y, Zr, Th and U are depleted in the greisens.

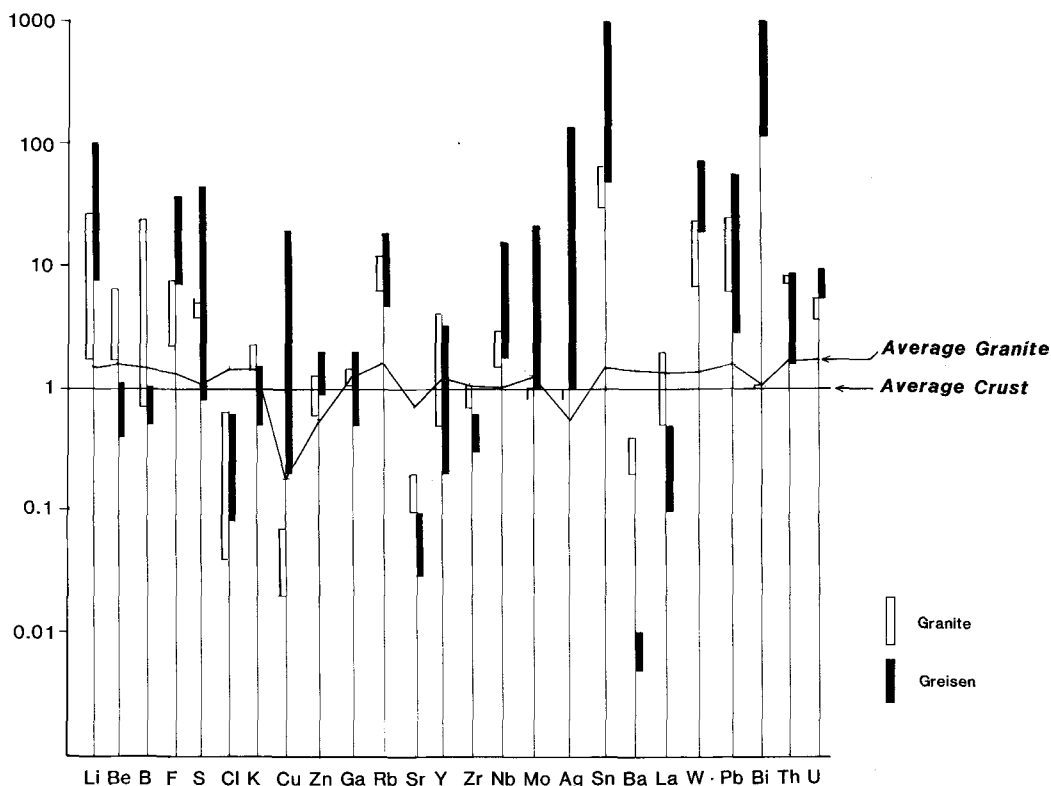


FIG. 5. Granite and greisen trace element patterns normalized to average crust (Taylor, 1964). Average granite (Taylor, 1964) is also shown.

Fluorine is enriched in the greisens over its granitic abundance and is fixed in mica, topaz and fluorite. Its levels fall within the range established by Bailey (1977) for greisens worldwide. However, it might be expected that large amounts of F, degassed from the cooling pluton, escaped upwards and outwards into the country rocks. Removal of Na and Ba during greisenization may have been effected by complexing with fluorine in a fluid phase.

Lastly it should be noted that sulphide mineralisation in the greisens has resulted in enhanced levels of Cu, Fe, Zn, Ag, Bi and Pb.

Veins. These are characterised by enhanced SiO_2 levels, reflecting the dominance of quartz, and correspondingly low levels of other major oxides.

The most noticeable trace element differences compared to the greisens are reduced Li and Rb, reflecting less mica, and the enhanced levels of sulphide and sulphosalt forming elements together with W.

Mineral chemical relations

Complex Nb-Ta oxides and wolframite. A variety of complex oxides of the form AB_2O_6 occur in the

granitic rocks and, as well as containing Ta and Nb, have substantial amounts of Ti, Sn, W and Sc. Ideally, *A*-site cations are divalent and *B*-site cations pentavalent giving rise to a columbite-type phase, e.g. FeNb_2O_6 . However, structural factors allow a wide range of coupled substitutions whereby elements such as Sn^{4+} and W^{6+} can be incorporated (Graham and Thornber, 1974), giving rise to more disordered ixiolitic varieties. Furthermore, there is a wide degree of chemical continuity with rutile (TiTi_2O_6).

Within the granite, ilmenorutiles contain a variable amount of Ta and Nb (Table 3). Rare W-rich ixiolite also occurs, indicating that W can be effectively fixed mineralogically within the granite and not released into residual fluids. In later pegmatitic differentiates, exemplified by sample 4005, ixiolite with variable chemistry occurs (Table 3) but exhibiting higher Mn/Fe, Ta/Nb, Sn and Sc than the granitic oxides.

The complex oxides described above are restricted to the magmatic rocks, whereas the greisens and veins are characterized by the presence of wolframite and cassiterite which indicates the ability of both Sn and W to survive as soluble complexes despite some fixation at the magmatic

TABLE 3. Nb - Ta oxide and wolframite analyses

Wt%	1	2	3	4	5	6	7	8	9
WO_3	32.43	1.37	15.66	12.67	4.44	7.09	76.82	77.47	77.04
Ta_2O_5	4.18	7.90	30.61	29.07	56.46	55.98	-	-	0.13
Nb_2O_5	38.29	23.37	29.33	30.09	8.15	17.29	0.54	0.02	0.74
TiO_2	3.04	51.97	3.62	3.31	7.53	10.54	-	-	-
SnO_2	1.10	2.65	1.96	8.50	9.26	6.41	0.01	-	-
Sc_2O_3	0.10	-	0.69	0.52	0.80	0.69	0.07	0.02	0.09
FeO*	14.10	10.46	4.19	4.85	4.62	4.94	17.07	6.62	15.35
MnO	5.07	0.02	11.92	10.54	8.19	7.72	5.76	17.83	7.20
Total	98.32	97.74	97.98	99.55	99.45	100.66	100.26	101.93	100.55

Atomic Proportions

W	0.542	0.017	0.278	0.221	0.085	0.131	1.001	0.992	1.000
Ta	0.073	0.106	0.570	0.533	1.129	1.083	0.000	0.000	0.000
Nb	1.117	0.520	0.908	0.917	0.271	0.234	0.012	0.000	0.017
Ti	0.147	1.924	0.186	0.168	0.416	0.564	0.000	0.000	0.000
Sn	0.028	0.052	0.054	0.228	0.271	0.182	0.000	0.000	0.000
Sc	0.006	0.000	0.041	0.031	0.051	0.043	0.003	0.001	0.004
Fe	0.761	0.431	0.240	0.273	0.284	0.294	0.718	0.274	0.643
Mn	0.277	0.001	0.691	0.602	0.510	0.465	0.245	0.747	0.305
O	6.000	6.000	6.000	6.000	6.000	6.000	4.000	4.000	4.000

Notes: 1: W-rich ixiolite, granite 4009. 2: Ilmenor tile, granite 4009.

3,4: Sn-rich ixiolites, pegmatite 4005. 5,6: Core, rim of tantalite, pegmatite 4005.

7: Wolframite 25.4% Huebnerite, vein 3412. 8,9: Wolframites 73.2, 32.2% Huebnerite, vein 4011.

* Total Fe

stage. Cassiterite is usually very close to pure SnO_2 , although trace amounts of Ta were noted which, together with other trace elements, accounts for the characteristic colour zoning in this mineral (Oen *et al.*, 1982).

Wolframites are generally opaque in thin section and correspondingly ferberitic (Table 3). However, minor amounts of a red translucent hubneritic variety also occur. Mn/Fe ratios are no longer regarded as simply temperature dependent (Groves and Baker, 1972), but can depend on wall-rock chemistry, oxygen fugacity and other intensive or extensive parameters. The generally constant Fe/Mn of most of the wolframites analysed suggests a wall-rock buffering condition applied in this case.

Other elements in the wolframites are in low abundance which indicates that most have been stabilized in earlier precipitating phases, with only small amounts of Nb available in the greisenizing fluids.

Micas. Micas occur in all the rock types described above and exhibit significant chemical variation. A problem in mica chemistry in this geologic context is the inability to determine Li using the electron

probe. In order to characterize the micas it is necessary to rely on Fe-Mg-Al relations, F contents and whole-rock Li values. A more detailed discussion of the micas in this and other similar occurrences is in preparation, thus only a summary account of their chemistry is presented here.

The extent of variation of the micas is shown in Fig. 6. The points plotted represent the average composition (Table 4) per sample based on up to 6 point analyses. It was found that intra-sample variation is small compared to the total variation and that this averaging is justified and simplifies the viewing of the data. The brown, optically homogeneous 'biotites' in the granites show quite a spread of composition and nowhere plot within the field of normal biotites as defined by Deer *et al.* (1962). They are better classified as siderophyllites and show a clear trend towards a theoretical zinnwaldite composition. Pale brown trioctahedral mica developed in a pegmatitic rock (4005) in fact plots almost exactly at the zinnwaldite point.

The greisen-hosted trioctahedral micas are optically rather variable with green-brown and colourless varieties. However, they plot as a restricted field close to zinnwaldite. The mica in the

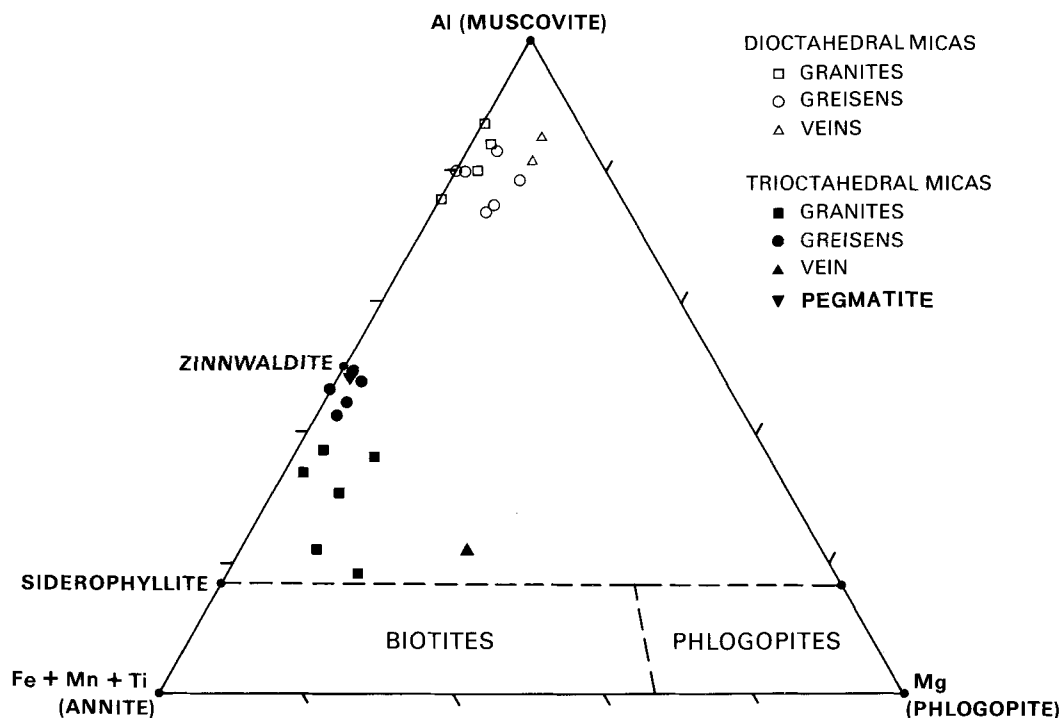


FIG. 6. Average mica compositions plotted in terms of octahedral Al-Mg-(Fe+Mn). Field of normal biotites and phlogopites from Deer *et al.* (1962) is shown together with the positions of theoretical end members.

TABLE 4. Trioctahedral Mica analyses

Wt%	GRANITES						PEGMATITE		GREISENS		
	4009	4059	4061	720	723	724	4005	4008	4010	4025	5003
SiO ₂	37.87	46.36	34.29	39.83	37.60	38.29	43.33	43.12	42.38	39.67	42.54
TiO ₂	1.80	1.21	2.25	1.04	2.85	0.96	0.14	0.10	0.00	0.18	0.41
Al ₂ O ₃	20.98	21.53	19.64	21.93	18.17	21.31	22.32	22.83	23.05	22.80	23.16
FeO*	21.69	18.40	23.77	22.11	24.18	23.85	14.50	17.51	19.15	19.37	20.18
MnO	0.86	1.15	0.66	0.50	0.27	0.51	3.73	1.08	0.77	1.29	0.58
MgO	2.02	2.24	4.01	0.74	2.28	0.49	0.47	0.72	0.79	0.71	-
CaO	0.23	0.13	0.09	-	-	-	0.38	0.00	0.06	0.07	0.09
Na ₂ O	-	0.46	1.01	0.09	0.20	0.10	0.48	0.41	0.57	0.71	-
K ₂ O	10.39	10.33	0.83	9.47	9.77	9.60	9.00	10.46	16.64	10.19	9.16
SnO ₂	0.08	0.07	0.02	0.12	0.05	0.03	0.02	0.03	0.02	0.02	ND
Nb ₂ O ₅	0.12	0.03	0.09	0.08	0.04	0.08	0.03	0.01	0.01	0.04	ND
F	1.45	3.35	1.26	1.81	1.26	1.24	2.99	2.15	1.03	3.03	1.36
Total	96.88	97.85	96.39	96.96	96.14	95.94	96.08	97.52	98.04	96.80	96.91

Atomic proportions

Si	5.766	6.017	5.367	5.989	5.827	5.885	6.399	6.304	6.183	5.994	6.241
Al ^{iv}	2.234	1.983	2.633	2.011	2.173	2.115	1.601	1.696	1.817	2.006	1.759
Al ^{vi}	1.531	1.800	0.990	1.875	1.146	1.745	2.284	2.238	2.147	2.054	2.246
Fe	2.762	2.294	3.111	2.780	3.134	3.065	1.791	2.141	2.337	2.448	2.476
Ti	0.206	0.136	0.275	0.118	0.332	0.111	0.016	0.011	0.000	0.020	0.045
Mn	0.111	0.145	0.097	0.064	0.035	0.066	0.467	0.134	0.095	0.165	0.072
Mg	0.458	0.498	0.935	0.166	0.527	0.112	0.103	0.157	0.172	0.160	-
Sn	0.005	0.004	0.001	0.007	0.003	0.002	0.001	0.002	0.001	0.001	-
Nb	0.008	0.002	0.006	0.005	0.003	0.006	0.002	0.001	0.001	0.003	-
Ca	0.038	0.021	0.015	-	-	-	0.060	-	0.009	0.011	0.014
Na	-	0.133	0.306	0.026	0.060	0.030	0.137	0.116	0.161	0.208	-
K	2.018	1.965	1.963	1.816	1.931	1.882	1.695	1.951	1.980	1.984	1.714
F	0.698	1.580	0.624	0.861	0.618	0.603	1.396	0.994	0.475	1.448	0.631
O	22.000	22.000	22.000	22.000	22.000	22.000	22.000	22.000	22.000	22.000	22.000

Notes: Average compositions based on several point analyses per sample

* Total Fe. ND = Not determined.

greisen sample 4025 is almost certainly a true zinnwaldite in that the rock is Li-rich and the colourless to light brown appearance of this mica corresponds to published optical data for zinnwaldite (Deer *et al.*, 1962). The rather more variably coloured micas in 4010 and 4008 cannot have more than about 1.0% Li₂O, given the whole-rock data, and may be better described as lithian siderophyllites.

The continuous trend in the trioctahedral micas suggests a continuous petrogenetic process of late-stage magmatic differentiation and greisenization. The Al content in mica may prove a sensitive indicator of the degree of evolution of such a process and also mineralization potential.

The 'vein' trioctahedral mica plotted in Fig. 6 is noticeably more magnesian than all the others.

This mica is developed in metawacke bordering an exocontact vein. It is distinctly F-rich, indicating metasomatism of the country rocks by volatile fluids passing along the vein system.

The dioctahedral micas (Table 5) show less variation and can all be classed as phengites. However, the granite phengites appear Mg-deficient compared to those in the greisens and veins. There do not appear to be significant changes in F content between the different rock types, although it is apparent that F partitions preferentially into the coexisting trioctahedral mica.

Age of intrusion and mineralization

Six whole-rock samples were analysed for Rb and Sr using standard techniques of X-ray fluor-

essence, with a precision of approximately 1.5% (1 sigma) on the Rb/Sr ratio due to the low concentration of Sr. Isotopic measurements were made using a VG Micromass 30 cm radius, 90° magnetic fields sector, mass spectrometer with on-line control. An isochron has been fitted to the data points using the two-error regression methods of York (1969).

TABLE 5. Representative Dioctahedral mica analyses

Wt%	4059	M0723	4008	4010	3412	4011
SiO ₂	46.45	48.15	45.83	47.93	46.32	47.58
TiO ₂	0.13	0.11	-	-	0.34	-
Al ₂ O ₃	29.45	30.05	32.21	31.64	30.04	31.94
FeO*	6.29	4.73	6.32	4.71	2.93	2.01
MnO	0.42	-	0.25	0.22	0.17	0.17
MgO	1.46	0.58	0.55	0.49	2.30	1.55
CaO	0.09	-	-	-	0.10	0.20
Na ₂ O	0.19	-	0.60	0.31	0.16	-
K ₂ O	11.18	10.65	11.13	11.44	11.23	11.22
SnO ₂	0.06	0.02	0.13	0.04	ND	ND
Nb ₂ O ₅	-	-	-	-	ND	ND
F	2.11	1.07	0.97	0.69	1.98	0.36
Total	96.94	94.91	97.58	97.18	94.74	94.88

Atomic Proportions

Si	6.371	6.571	6.197	6.419	6.381	6.417
Al ^{iv}	1.629	1.429	1.803	1.581	1.619	1.583
Al ^{vi}	3.131	3.404	3.330	3.413	3.258	2.923
Fe	0.721	0.540	0.715	0.527	0.338	0.227
Ti	0.013	0.011	-	-	0.035	-
Mn	0.049	-	0.029	0.025	0.020	0.019
Mg	0.298	0.118	0.111	0.098	0.472	0.312
Sn	0.003	0.001	0.007	0.002	-	-
Nb	-	-	-	-	-	-
Ca	0.013	-	-	-	0.015	0.029
Na	0.051	-	0.157	0.080	0.043	-
K	1.956	1.854	1.920	1.954	1.083	1.930
F	0.915	0.462	0.415	0.292	0.863	0.134
O	22.000	22.000	22.000	22.000	22.000	22.000

Notes: Average compositions based on several point analyses.

* Total Fe. ND = Not determined.

K-Ar ratios were obtained on biotites and K-feldspar from two of the six samples (Table 6). K was determined in duplicate by flame photometry, using Li as an internal standard. Ar ratios were determined by isotope dilution using a VG Micromass 1200 spectrometer with Ar tracer or spike. Errors are quoted at the two sigma level.

The Rb-Sr isochron (Fig. 7) gives an age of crystallization of 80 ± 1 Ma (Late Cretaceous) with an initial ratio of 0.7151 ± 0.0006 . The biotite K-Ar ages similarly confirm an age of 80 Ma, although K-feldspar indicates loss of radiogenic Ar due to a

TABLE 6. Whole-rock and mineral isotope data

Whole-rock Rb-Sr data		
Sample no.	⁸⁷ Rb/ ⁸⁶ Sr	⁸⁷ Sr/ ⁸⁶ Sr
M0719	173.89±1.5%	0.90247±0.004%
M0720	167.44±1.5%	0.90202±0.012%
M0721	152.40	0.88250±0.010%
M0722	204.01	0.92852±0.007%
M0723	24.65	0.74293±0.005%
M0724	223.53	0.95466±0.005%

Mineral K-Ar data

Sample no.	Mineral	%K	vol. rad ⁴⁰ Ar	Age ± 2 sigma
M0719	Biotite	7.19	22.39 nl/g	79 ± 2 Ma
M0719	K-feldspar	10.63	27.00	64 ± 2
M0723	Biotite	6.92	21.36	78 ± 2
M0723	K-feldspar	10.07	29.19	73 ± 2
4059	Biotite	7.97	25.1	79 ± 2
4061	Biotite	6.64	21.3	81 ± 2

Note: K-Ar determinations on 4059 and 4061 financed through the good offices of P.T. Caltex Pacific Indonesia.

mild reheating event, corresponding possibly to clouding and sericitization of the feldspars.

Mineralization around the margins of the pluton is demonstrably related to greisenization which in turn can be ascribed to veining by reactive fluids. Ore minerals in the veins are similar to those in the greisens and there is a continuity in mica chemistry between the end stages of granite and pegmatite crystallization and greisen. All this points to the contention that the greisens formed by granite autometasomatism, the fluids possibly driven outwards and upwards from the still consolidating pluton and reacting with the already crystallized margins. There is no evidence for a significant time

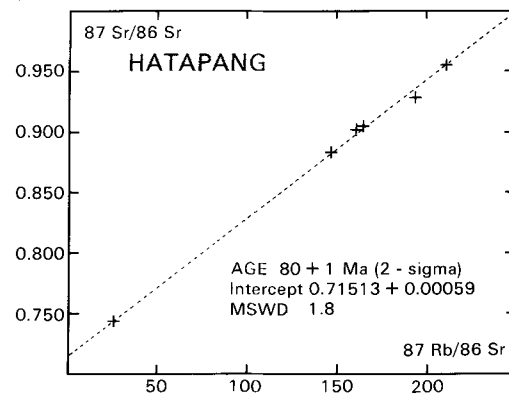


FIG. 7. Rb-Sr whole-rock isochron for the Hatapang granite. Half-life constants as recommended by Steiger and Jaeger (1977).

break between intrusion and the onset of greisenization and mineralization.

Granite classification and tectonic setting

S-type granitoids as defined by Chappell and White (1974) are characterized by high Al, giving rise to primary white mica and normative corundum, high K_2O/Na_2O and high initial strontium ratios (> 0.708). They are also compositionally more restricted to the high silica end of the igneous spectrum than I-type granitoids. The Hatapang as described above is clearly S-type and shows no transitional features, as many granites do, with the I-type class. The broadly parallel dual classification of Ishihara (1977) separates granitoids into ILMenite and MAGnetite series, the former reflecting a crustal anatexis origin by virtue of low abundances of opaque oxides and corresponding low states of iron oxidation ($Fe_2O_3/FeO < 0.5$) and again the Hatapang granite (Table 1) falls neatly into the ILM-series. Both ILM and S-type granites are believed to indicate the presence of thickened crust in an orogenic belt and are characteristically associated with Sn-W greisens.

Similarly, Pitcher's (1983) criteria for the Hercynotype or S-type granitoid neatly encompasses those features of the Hatapang granite and its geologic environment. This can be illustrated using trace element Rb, Ba, Sr and K as in Figs. 8 and 9. The Hercynotype representatives (the Cornubian

granites and Hatapang) are characterized by low Ba and Sr and by lower K/Rb ratios compared to the Cordilleran (I-type) or Alpine (M-type) granitoids. The geochemically similar A-type or Nigerian granitoid can be easily distinguished by geologic setting and peralkaline characteristics.

Genesis of Sn-W mineralisation

Groves (1972) and Groves and Taylor (1973) have shown that Sn and W mineralization is related to the most highly fractionated members of a batholithic series, as indicated particularly by the low levels of Ba and Sr and high Rb. The incompatible elements Sn, W, Nb, U, Th, Li and Be are also enriched in the residual magmas and for the most part crystallize in the evolved granites in various accessory phases such as described above occurring in the Hatapang granite. Studies of silicic ash-flow tuffs, such as the Bishop Tuff (Hildreth, 1981), show that extreme enrichment of water, halogens and some alkalis, together with W, Nb, Sn, Th, U, Li, Be and Ta, occur within the roof zone of the magma chamber. Elements such as Ba, Sr and La are by contrast strongly depleted. Crystal-liquid fractionation, liquid-state diffusion and halogen complexing in the hydrous fluid have been invoked to account for these patterns (Hildreth, 1981; Leat *et al.*, 1984), which are clearly analogous to those in Sn-W greisens (cf. Fig. 5).

In the batholithic environment segregation of

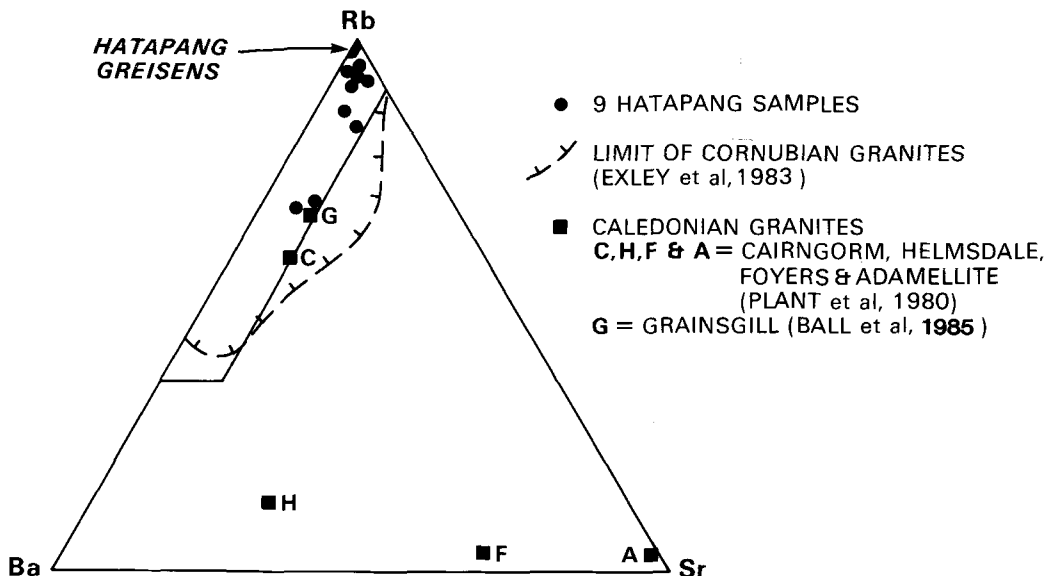


FIG. 8. Rb-Sr-Ba relations for the Hatapang and other plutons in relation to the field of highly differentiated granites of El Bouseily and El Sokkary (1975).

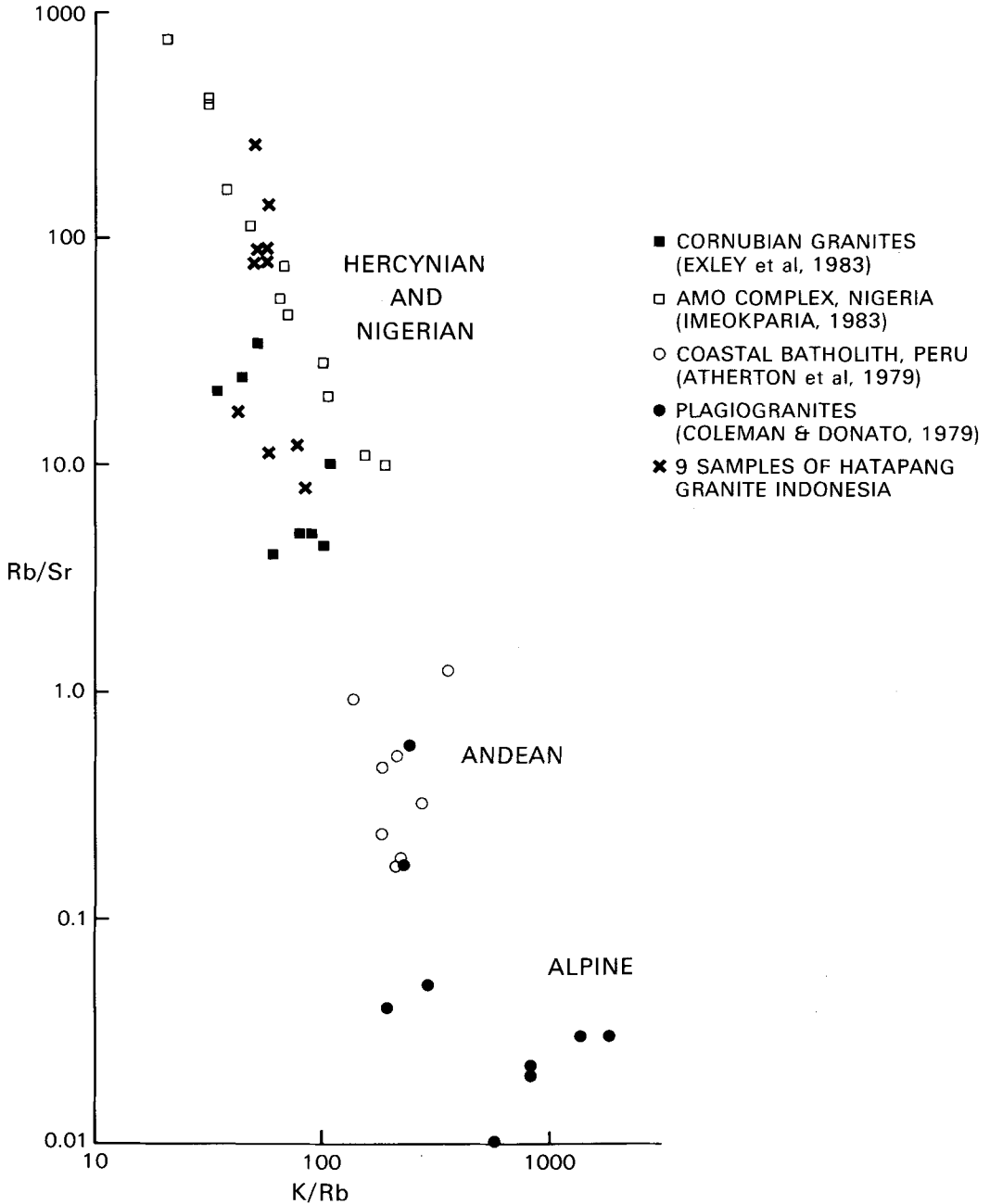


Fig. 9. Rb/Sr-K/Rb plot showing the Hatapang granite in relation to granites of various regional settings.

residual, volatile-rich fluids occurs as the batholith cools and as these migrate toward the roof and margins of a pluton, the fluids will react, being in disequilibrium with earlier crystallized granite and

country rock. Extensive hydrofracturing due to increased fluid pressure occurs concurrently, allowing the establishment of a widespread hydrothermal circulation. This leads to the formation of

F-rich greisens, veins and sheet-like apophyses penetrating the country rock (cf. Groves and McCarthy, 1978). During these processes, the Hatapang data shows that some of the elements enriched by magmatic differentiation are essentially fixed at the end-magmatic stage, for example Nb and Ta in pegmatitic ixiolite. Others, particularly Sn and W, whilst incorporated in accessory phases and mica, persist as complexes in late-stage and post-magmatic hydrous fluids and are deposited in quartz veins and their greisen borders. In terms of the temperatures of mineralization, Fig. 4 indicates that magmatic crystallization ceases below about 680°C. Greisens must have finally stabilized below about 600°C, at 1 kbar, which is the upper stability temperature for the muscovite + quartz assemblage.

It seems likely that F complexing is important for the transport of Sn and W with the deposition of cassiterite and wolframite perhaps triggered by the fixation of F in mica, topaz and fluorite. Cl, the other potential complexing anion (e.g. Eugster, 1985) is in very low abundance in the granites and greisens and seems unlikely to have been important at this stage. Preliminary fluid inclusion studies on wolframite-bearing quartz veins at Hatapang indicate that CO₂-rich fluids are significant, and the segregation of wolframite from cassiterite deposition suggests that carbonyl complexes may be important in W mobility. Shepherd and Waters (1984) note that CO₂-rich inclusions are a diagnostic feature of other tungsten deposits.

The associated sulphide mineralization post-dates and is of lower temperature than the Sn-W oxide phase. This involves the elements Ag, Bi, Cu, Pb, As and Zn, none of which are noticeably enriched in the host granites. Cu, Ag and Zn, in particular, show antipathetic behaviour in silicic magma chambers to the Sn, W, Nb and Ta group of elements (Hildreth, 1981). Thus it is not clear where the sources of these elements are to be found although the sulphide suite is entirely typical of other granite hosted Sn-W deposits (e.g. China—Tanelli, 1982; Brazil—Oen *et al.*, 1982; Missouri—Lowell and Gasparrini, 1982). It seems probable, though, that these elements were scoured from the country rocks by circulating fluids of magmatic and/or meteoric origin.

Regional setting and economic implications

As Suryono and Clarke (1982) have noted, the discovery of a substantial granite-related Sn-W deposit at Hatapang has important implications regarding the extent of the SE Asian tin province. Conventionally this includes Burma, Thailand, peninsular Malaysia and the Bangka-Billiton

group of islands to the east of Sumatra. Mainland Sumatra did not easily relate to this belt, largely through ignorance of its geology as indicated by figures in the publications of Hutchinson and Taylor (1978) and Hosking (1977). A few cassiterite localities were known in Sumatra and Hosking (1977) tentatively classes them as a displaced portion of the western belt. However, as Suryono and Clarke (1982) suggest, the occurrence of Sn and W mineralization in Sumatra is controlled by the exposure of the pre-Tertiary basement in which Hatapang and other localities are emplaced. Basement exposure in turn is related to uplift in the Tertiary and Quaternary which is a function of subduction parallel to the west coast of Sumatra. Any connection with the main tin belt is obscured by recent back-arc basin development. A proposed revision of the distribution of the various belts is illustrated in Fig. 10.

Several features indicate that the Hatapang occurrence should be correlated with the Ii portion of the western belt (Fig. 10). Foremost among these is the Cretaceous age of the Hatapang pluton. This differs significantly from the Triassic age of the Main range (Fig. 10) and eastern belts. Hatapang is clearly more akin to, although slightly younger than, the predominantly Middle Cretaceous ages found within the westernmost belt, such as at Phuket and Khao Daen (Beckinsale, 1979). The Thai-Burmese granites of this belt are also emplaced in similar glacio-marine continental type sediments to the Sumatran Tapunuli Group. Other features such as the close association of W with Sn, the red-brown pleochroism of cassiterite, and the occurrence of Nb-Ta pegmatitic species, are characteristic of Hatapang and have been shown to distinguish the western from the Main range and eastern belts (Hutchinson and Taylor, 1978; Hosking, 1977).

Cretaceous granites of the westernmost belt (as shown in Fig. 10) include both S and I-types and result from an event separate in both space and time from the Permo-Trias Main range and eastern belts. These older granites are separated by the Bentong-Raub suture and their generation can be ascribed to continental collision tectonism at this time. Generation of the later, Cretaceous, granites can be equated with the establishment of a back-arc fold-thrust belt (Mitchell, 1979) involving ensialic basinal sediments, and due to easterly dipping subduction of Indian oceanic crust (cf. Beckinsale, 1979). In mainland Sumatra at this time oblique subduction of the Indian oceanic plate led to the destruction of a Mesozoic marginal basin assemblage along the line now represented by the Sumatran Fault System (Cameron *et al.*, 1980).

Presently, virtually all the Sn and W production

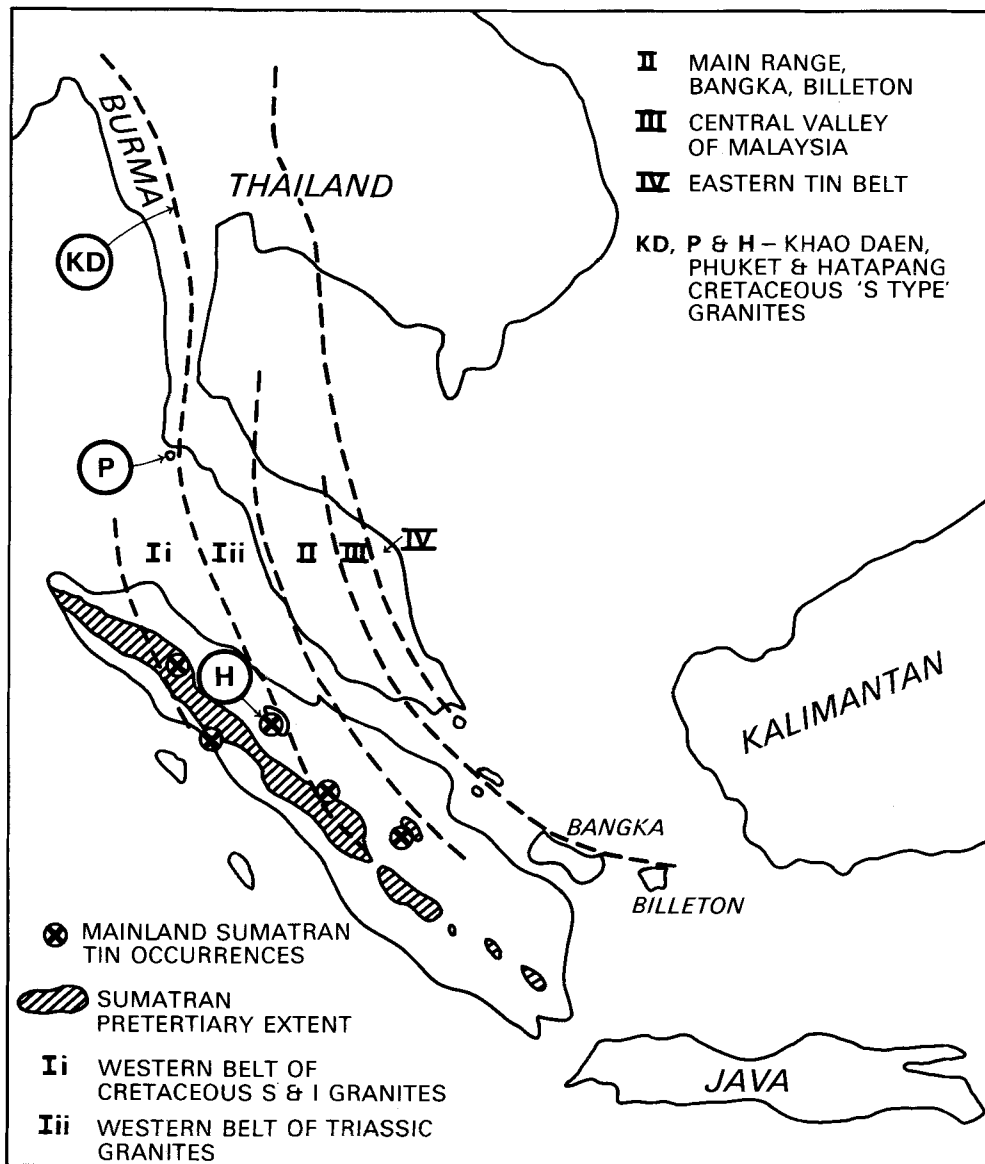


FIG. 10. Possible correlation of Sumatra with the SE Asia mineralized plutonic belts. Modified after Mitchell (1979), Hutchinson and Taylor (1978), and Beckinsale (1979).

from Indonesia is related to granites forming the Bangka and Billiton group of islands east of Sumatra, and which are characteristic of the Main range and eastern belts in which W is very subordinate to Sn. The recognition within mainland Sumatra of tin granites of the younger western belt, in which W mineralisation is recognised to be relatively more important, offers confirmation that

the terrain east of the Sumatra Fault Zone (Fig. 1) is a continuation of the crustal block containing the SE Asian tin province. This in turn indicates that the mineral potential of the basement forming this part of Sumatra is greater than hitherto thought. Despite recent advances in the geological knowledge of Sumatra it can be fairly certain that only a fraction of this mineral potential has been realised.

Acknowledgements

This study was financed in part by the Overseas Development Administration under its UK aid programme to Indonesia. We thank our colleagues in BGS for helpful discussion and encouragement, in particular Drs J. F. W. Bowles and T. J. Shepherd. M. Brook is especially thanked for contributing the K-Ar and Rb-Sr isotopic data. The study would not have been possible without the cooperation of personnel of the Directorate of Mineral Resources, Indonesia (Director: Ir. Salman Padmanagara). This paper is published with the permission of the Director, British Geological Survey (NERC).

References

- Atherton, M. P., McCourt, W. J., Sanderson, L. M., and Taylor, W. P. (1979) The geochemical character of the segmented Peruvian Coastal batholith and associated volcanics. In *Origin of granite batholiths—geochemical evidence* (Atherton, M., and Tarney, J., eds.). Shiva, 45–64.
- Bailey, J. C. (1977) Fluorine in granitic rocks and melts: a review. *Chem. Geol.* **19**, 1–42.
- Ball, T. K., Fortey, N. J., and Shepherd, T. J. (1985) Mineralisation at the Carrock Fell tungsten mine, N. England: Paragenetic, fluid inclusion and geochemical study. *Mineral. Deposita*, **20**, 57–65.
- Beckinsale, R. D. (1979) Granite magmatism in the tin belt of Southeast Asia. In *Origin of granite batholiths—geochemical evidence* (Atherton, M. P., and Tarney, J., eds.). Shiva, 34–44.
- Cameron, N. R., Clarke, M. C. G., Aldiss, D. T., Aspden, J. A., and Djunuddin, A. (1980) The geologic evolution of northern Sumatra. *Proc. 9th Ann. Conf. Indon. Petrol. Assoc., Jakarta*. 149–87.
- Chappell, B. W., and White, A. J. R. (1974) Two contrasting granite types. *Pacific Geol.* **8**, 173–4.
- Clarke, M. C. G., Ghazali, S. A., Harahap, H., Kusyono, and Stephenson, B. (1982) *The geology of the Peman-tangsiantar Quadrangle, Sumatra (with map)*. Geol. Res. Dev. Centre, Bandung.
- Coleman, R. G., and Donato, M. M. (1979) Oceanic plagiogranite revisited. In *Trondjemites, dacites and related rocks* (Barker, F., ed.). Elsevier, 149–68.
- Deer, W. A., Howie, R. A., and Zussman, J. (1962) *Rock forming minerals*. Vol. 3 (Sheet silicates). Longmans.
- El Bouseily, A. M., and El Sokkary, A. A. (1975) The relation between Rb, Ba and Sr in granitic rocks. *Chem. Geol.* **16**, 207–19.
- Eugster, H. (1985) Granites and hydrothermal ore deposits: a geochemical framework. *Mineral. Mag.* **49**, 7–23.
- Exley, C. S., Stone, M., and Floyd, P. A. (1983) Composition and petrogenesis of the Cornubian granite batholith and post-orogenic volcanic rocks in Southwest England. In *The Variscan fold belt in the British Isles* (Hancock, P. L., ed.). Hilger, 153–77.
- Graham, J., and Thornber, M. R. (1974) The crystal chemistry of complex niobium and tantalum oxides. 1: Structural classification. *Am. Mineral.* **59**, 1026–39.
- Groves, D. I. (1972) The geochemical evolution of tin-bearing granites in the Blue Tier Batholith, Tasmania. *Econ. Geol.* **67**, 445–57.
- and Baker, W. E. (1972) The regional variation in composition of wolframites from Tasmania. *Ibid.* **67**, 362–8.
- and McCarthy, T. S. (1978) Fractional crystallisation and the origin of tin deposits in granitoids. *Mineral. Deposita*, **13**, 11–26.
- and Taylor, R. G. (1973) Greisenisation and mineralisation at Anchor tin mine, northeast Tasmania. *Trans. Inst. Mining Metall.* **82**, B135–46.
- Hamidsyah, H., and Clarke, M. C. G. (1982) Discovery of primary tungsten and tin mineralisation in North Sumatra, Indonesia. In *Symposium on tungsten geology* (Hepworth, J. V., and Yu Hong Zhang, eds.). ESCAP/RMRDC (UN), China, 49–58.
- Hildreth, W. (1981) Gradients in silicic magma chambers: Implications for lithospheric magmatism. *J. Geophys. Res.* **86B**, 10153–92.
- Hosking, K. F. G. (1977) Known relationships between the 'hard rock' tin deposits and the granites of Southeast Asia. *Geol. Soc. Malaysia Bull.* **9**, 141–57.
- Hutchinson, C. S., and Taylor, D. (1978) Metallogenesis in SE Asia. *J. Geol. Soc. London*, **135**, 407–28.
- Imeokparia, E. G. (1983) Geochemical aspects of the evolution and mineralisation of the Amo Younger Granite Complex (northern Nigeria). *Chem. Geol.* **40**, 293–312.
- Ishihara, S. (1977) The magnetite-series and ilmenite-series granitic rocks. *Min. Geol. Japan*, **27**, 293–305.
- Johari, S., Clarke, M. C. G., Djunuddin, A., and Stephenson, B. (1981) New evidence of tin and tungsten mineralisation in northern Sumatra. *Proc. 4th Reg. Conf. Geol. SE Asia*. Geol. Soc. Philippines, 497–508.
- Leat, P. T., MacDonald, R., and Smith, R. L. (1984) Chemical evolution of the Menengai caldera volcano, Kenya. *J. Geophys. Res.* **89B**, 8571–92.
- Lowell, G. R., and Gasparrini, C. (1982) Composition of arsenopyrite from topaz greisen veins in southeast Missouri. *Mineral. Deposita*, **17**, 229–38.
- Manning, D. A. C., Hamilton, D. L., Henderson, C. M. B., and Dempsey, M. J. (1980) The probable occurrence of interstitial Al in hydrous F-bearing and F-free aluminosilicate melts. *Contrib. Mineral. Petrol.* **75**, 257–62.
- Metcalfe, I. (1983) Conodont faunas, age and correlation of the Alas Formation (Carboniferous), Sumatra. *Geol. Mag.* **120**, 579–86.
- Mitchell, A. H. G. (1979) Rift, subduction and collision related tin belts. *Geol. Soc. Malaysia Bull.* **11**, 81–102.
- Oen, I. S., Korpershoek, H. R., Kieft, C., and Lustenhouwer, W. J. (1982) A microprobe study of rutile, cassiterite, wolframite and sulphides in the Mono Potosi greisen, Rondonia, Brazil. *Neues Jahrb. Mineral. Mh.* 175–91.
- Page, B. G. N., Bennett, J. D., Cameron, N. R., Bridge, D. McC., Jeffrey, D. H., Keats, W., and Thab, J. (1978) Regional geochemistry and geological reconnaissance mapping and mineral exploration in northern Sumatra,

- Indonesia. *Proc. 11th Common. Min. Metall. Congr., Hongkong*, 455-62.
- Pitcher, W. S. (1983) Granite type and tectonic environment. In *Mountain building processes* (Hsu, K., ed.). Academic Press, 19-40.
- Plant, J. A., Brown, G. C., Simpson, P. R., and Smith, R. T. (1980) Signatures of metalliferous granites in the Scottish Caledonides. *Trans. Inst. Mining Metall.* **89**, B198-210.
- Shepherd, T. J., and Waters, P. (1984) Fluid inclusion gas studies, Carrock Fell tungsten deposit, England: Implications for regional exploration. *Mineral. Deposita*, **19**, 304-14.
- Stephenson, B., Ghazali, S. A., and Widjaja, H. (1982) *Regional geochemical atlas series of Indonesia*, 1. BGS, Keyworth, UK.
- Steiger, R. H., and Jaeger, E. (1977) Subcommittee on geochronology: Convention on the use of decay constants in geocosmochronology. *Earth Planet. Sci. Lett.* **36**, 359-62.
- Streckeisen, A. L. (1976) To each plutonic rock its proper name. *Earth Sci. Rev.* **12**, 1-33.
- Suryono and Clarke, M. C. G. (1982) Primary tungsten occurrences in Sumatra and the Indonesian tin islands. In *Symposium on tungsten geology* (Hepworth, J. V., and Yu Hong Zhang, eds.). ESCAP/RMRDC (UN), China, 217-31.
- Tanelli, G. (1982) Geological setting, mineralogy and genesis of tungsten mineralisation in the Dayu district, Jiangxi (People's Republic of China): An outline. *Mineral. Deposita*, **17**, 279-94.
- Taylor, S. R. (1964) Abundance of chemical elements in the continental crust: A new table. *Geochim. Cosmochim. Acta*, **28**, 1273-85.
- York, D. (1969) Least squares fitting of a straight line with correlated errors. *Earth Planet. Sci. Lett.* **5**, 320-4.

[Manuscript received 28 May 1986;
revised 10 November 1986]